Estuaries and Coasts (2014) 37:1532–1548
DOI 10.1007/s12237-014-9796-3

Thresholds of Adverse Effects of Macroalgal Abundance and Sediment Organic Matter on Benthic Habitat Quality in Estuarine Intertidal Flats

Martha Sutula · Lauri Green · Giancarlo Cicchetti · Naomi Detenbeck · Peggy Fong

Received: 5 November 2012 / Revised: 23 January 2014 / Accepted: 28 February 2014 / Published online: 18 March 2014

Abstract Confidence in the use of macroalgae as an indicator of estuarine eutrophication is limited by the lack of quantitative data on the thresholds of its adverse effects on benthic habitat quality. In the present study, we utilized sediment profile imagery (SPI) to identify thresholds of adverse effects of macroalgal biomass, sediment organic carbon (% OC) and sediment nitrogen (% N) concentrations on the apparent Redox Potential Discontinuity (aRPD), the depth that marks the boundary between oxic near-surface sediment and the underlying suboxic or anoxic sediment. At 16 sites in eight California estuaries, SPI, macroalgal biomass, sediment percent fines, % OC, and % N were analyzed at 20 locations along an intertidal transect. Classification and Regression Tree (CART) analysis was used to identify step thresholds associated with a transition from "reference" or natural background levels of macroalgae, defined as that range in which no effect on aRPD was detected. Ranges of 3–15 g dw macroalgae m^{-2}, 0.4–0.7 % OC and 0.05–0.07 % N were identified as transition zones from reference conditions across these estuaries. Piecewise regression analysis was used to identify exhaustion thresholds, defined as a region along the stress–response curve where severe adverse effects occur; levels of 175 g dw macroalgae m^{-2}, 1.1 % OC and 0.1 % N were identified as thresholds associated with a shallowing of aRPD to near zero depths. As an indicator of ecosystem condition, shallow aRPD has been related to reduced volume and quality for benthic infauna and alteration in community structure. These effects have been linked to reduced availability of forage for fish, birds and other invertebrates, as well as to undesirable changes in biogeochemical cycling.

Keywords Macroalgae · Eutrophication · Thresholds · Sediment profile imaging · Benthic habitat quality · Percent organic carbon · Percent nitrogen

Communicated by Marco Bartoli

Electronic supplementary material The online version of this article (doi:10.1007/s12237-014-9796-3) contains supplementary material, which is available to authorized users.

M. Sutula (✉)
Southern California Coastal Water Research Project, 3535 Harbor Boulevard, Costa Mesa, CA 92626, USA
e-mail: marthas@sccwrp.org

L. Green · P. Fong
Department of Evolutionary Biology and Ecology, University of California, Los Angeles, 621 Charles E. Young Drive, South, Los Angeles, CA 90095-1606, USA

G. Cicchetti · N. Detenbeck
U.S. EPA Office of Research and Development, National Health and Environmental Effects Research Laboratory, Atlantic Ecology Division, 27 Tarzwell Drive, Narragansett, RI 02882, USA

Introduction

Marine macroalgae form an important component of highly diverse ecosystems in estuaries worldwide and, in moderate abundances, provide vital ecosystem services (Fong 2008). However, some species of macroalgae thrive in nutrient-enriched waters, forming extensive blooms in intertidal and shallow subtidal habitats. These macroalgal blooms can outcompete other primary producers, at times completely blanketing the seafloor and intertidal flats. This results in hypoxia and reduced abundance and diversity of benthic invertebrates, leading to trophic level effects on birds and fish and disruption of biogeochemical cycling (Sfriso et al. 1987; Valiela et al. 1992, 1997; Raffaelli et al. 1989; Bolam et al. 2000). The causal mechanisms for adverse effects on benthic invertebrates have been well studied; labile organic matter associated with macroalgal blooms stimulates the bacterial communities in sediments, increasing benthic oxygen demand (Sfriso et al. 1987; Lavery and McComb 1991), and

decreasing sediment redox potential (Cardoso et al. 2004). Zones of sediment anoxia and sulfate reduction become shallow, often extending throughout the sediment under the algal mat (Dauer et al. 1981; Hentschel 1996). This leads to pore water ammonia and sulfide concentrations that are toxic to surface deposit feeders (Giordani et al. 1997; Kristiansen et al. 2002).

While many studies have documented these effects, few have been conducted with the expressed intent of informing thresholds of adverse effects of macroalgae. Several studies have used controlled field experiments to show causal effects of manipulated macroalgal biomass and duration on benthic infaunal abundance and diversity (Norkko and Bonsdorff 1996; Cummins et al. 2004; Green 2010; Green et al. 2013). While these studies provide well-documented benchmarks of adverse effects, collectively they have the drawback that the findings are most applicable in the estuaries in which the experiments were conducted. It is difficult to extrapolate these experimental results to other estuaries that may vary with respect to climate, hydrology, and sediment characteristics, all of which could influence the susceptibility of benthic habitat to macroalgal blooms. Further, even in the most comprehensive of these studies, a large gap exists among biomass treatments in which observed no-effect and effect levels occurred (0–125 g dry weight [dw] m^{-2}; Green et al. 2013), leaving room for refinement in understanding of where the actual thresholds may be occurring. Field surveys allow us to capture a wider gradient of condition and can help to fill this gap. The one example of this that is relevant for threshold investigation is Bona (2006), who conducted a field survey of effects of macroalgal abundance on benthic habitat quality using sediment profile imaging (SPI). However, this work was conducted in one estuary, and was not intended for applicability across a wide range of estuarine gradients. Use of macroalgal indicators is increasing in regional and national assessments of estuarine eutrophication (Bricker et al. 2008; McLaughlin et al. 2013). Consequently, an improved understanding of thresholds across estuaries will help to refine the methods with which these assessments are made (Bricker et al. 2003; Scanlan et al. 2007; Borja et al. 2011).

Ecological thresholds have been defined as “the point at which there is an abrupt change in an ecosystem property or where small changes in an environmental driver produce large responses in the ecosystem” (Groffman et al. 2006). Ecological thresholds have also been associated with the concept of resilience and a transition between alternate stable states (Resilience Alliance and Santa Fe Institute 2004). These state changes may be associated with abrupt changes in one or more response variable as a key driver crosses a threshold value. Cuffney et al. (2010) further distinguish between resistance thresholds (e.g., a sharp decline in ecosystem condition following an initial no effect zone) and exhaustion thresholds (a sharp transition to zero slope at the end of a stressor gradient at which point the response variable reaches a natural limit). In contrast to resistance or exhaustion thresholds, we define “reference envelope" as the physical, chemical or biological characteristics of sites found in the best available condition according to the response variable of interest (Stoddard et al. 2006), since few California estuaries have been untouched by human disturbance. As defined by Cuffney et al. (2010), resistance and exhaustion thresholds are both examples of slope thresholds. Change point or step-like thresholds have also been used to detect reference and non-reference populations, denoting an abrupt discontinuity in magnitude of a response variable along a stressor gradient, but not necessarily associated with a change in slope (Qian et al. 2003).

SPI technology has long been used to rapidly evaluate benthic habitat quality (Rhoads and Cande 1971; Rhoads and Germano 1986). SPI technology uses a camera system with a wedge-shaped prism that penetrates into and images a vertical profile of sediments (Rhoads and Cande 1971). The typical use of SPI data in subtidal sediments calculates a multi-metric index based on indicators ranging from reduced gas bubbles, stage of benthic colonization, various faunal features, and apparent Redox Potential Discontinuity (aRPD), i.e., the boundary between the lighter brown or reddish sub-oxic near-surface sediment and the underlying grey or black anoxic sediment (Rhoads and Germano 1982; Nilsson and Rosenberg 1997; Teal et al. 2009). The lower limit of the aRPD represents the Fe redox boundary, a reduced environment where reductive dissolution of iron occurs (Teal et al. 2009). SPI has rarely been conducted in intertidal habitat, where macroalgae are typically assessed (e.g., Bona 2006). Many typical SPI indicators, such as gas bubbles and stage of colonization, are not applicable in this habitat type. The aRPD, which approximates the extent of oxygen penetration into the sediment and the vertical extent of infaunal activity within the sediment, is a reliable response indicator for organic matter enrichment in sediments and is applicable to intertidal habitat.

The objectives of this study were to: (1) document the relationships between macroalgal biomass and cover, sediment organic matter and nutrients, and benthic habitat quality measured through aRPD across a range of eight enclosed bays and coastal lagoons in California and (2) identify thresholds or tipping points in benthic habitat quality in these data as well as the reference envelope where the likelihood of adverse effects are low. We hypothesized that, following an initial no effect zone (reference envelope), we would see a sharp decline in aRPD with increasing macroalgal biomass and

sediment organic matter, ultimately declining to near zero (exhaustion threshold).

Materials and Methods

Conceptual Approach

For this study, we used SPI technology to rapidly evaluate benthic habitat quality directly associated with macroalgal abundance (Bona 2006). We chose to focus on estuarine intertidal flats as the targeted habitat type for this study, as monitoring of macroalgae is most cost-effective in this zone (Scanlan et al. 2007). The camera can be deployed rapidly, which allowed us to survey a wide range of conditions within and across estuaries. Macroalgal biomass and sediment percent organic carbon (% OC) and nitrogen (% N) content served as independent variables in our analyses, while aRPD served as the univariate response variable. The depth of aRPD is well correlated with a number of co-varying factors including bottom-water DO concentrations (Diaz et al. 1992; Cicchetti et al. 2006), faunal successional stage (Pearson and Rosenberg 1978; Rosenberg et al. 2003), bioturbation (Pearson and Rosenberg 1978; Rhoads and Germano 1982), sediment carbonate, iron, aluminum content and % OC (Rosenberg et al. 2003; Viaroli et al. 2010), and physical energy (Rhoads and Germano 1982). We interpret aRPD for this paper as "a reasonable approximation of benthic ecosystem functioning … [that] is highly context driven" (Teal et al. 2010), within our context of estuarine intertidal flats on the west coast of the United States.

Study Area and Site Selection

The California Coast extends from the Smith River (41.46°N) to the U.S.–Mexico border (32.53°N; Fig. 1). Along this 1,700-km coastline, a temperate climate exists north of Cape Mendocino with a moderate Mediterranean climate to the south. Average annual air temperatures and rainfall range from 15 °C and 967 mm of rainfall in the north to 19 °C and 262 mm in the south. Rainfall along the coast is concentrated largely over the fall through late spring.

Among California's diverse array of estuaries, "bar-built" lagoonal and river mouth estuaries are the most numerous, a type of estuary named for the formation of sandbars that build up along the mouth as a consequence of longshore sediment transport and seasonally low freshwater discharge (Ferren et al. 1996). Bar-built estuaries are usually shallow (<2 m), with reduced tidal action during time periods when the sand bar restricts tidal exchange, typically during periods of low freshwater input (Largier and Taljaard 1991).

We selected 16 sites in eight bar-built estuaries along the California coast that were open to tidal exchange at the time (Table 1). Within each estuary, one to three intertidal sites were selected along the longitudinal axis of the estuary (Fig. 1; Table 1).

Field Sampling and Laboratory Methods

Field measurements were conducted in the months of August–September 2011. At each site within an estuary, a 20-m transect was established in the lower intertidal zone along the same elevational contour at 0.3–0.6 m above MLLW. Within each transect, percent cover and biomass of macroalgae were estimated at 20 randomly chosen 0.0625-m^2 plots. Cover was estimated using the point intercept method. Biomass was harvested and stored on ice until processing. At each plot where biomass was collected, an 8-megapixel SPI camera (Konica-Minolta Dimage A2.e constructed by USEPA, 15 cm viewed width) was inserted manually into the sediment to 15 cm depth, and a digital image of the sediment cross section was taken. In addition, at each point a core (12.5 cm inner diameter, 2 cm deep) of surface sediments was taken for analysis of grain size, % OC, and % N.

In the laboratory, macroalgal biomass samples were cleaned, sorted to genus and wet weighed, then dried and reweighed. The weights of all macroalgal genera were summed for each quadrat and normalized over the area of the biomass sampled to give a total macroalgal wet weight, dry weight, and percent composition by genus in each quadrat. A least squares regression between wet and dry weight biomass was calculated by genus and group to make our results, presented in dry weight, comparable to other studies which report findings in wet weight (Table S1). Dried sediment was ground with a mortar and pestle for analysis of % N and % OC measured by high temperature combustion on a Control Equipment Corp CEC 440HA elemental analyzer (University of California Marine Science Institute, Santa Barbara, CA). The remainder of the sediment was wet sieved through a 65 μm sieve to determine percent fines.

SPI imagery was transferred to a computer and the lighter tan, brown, or red aRPD area was digitized using Adobe Photoshop CS Version 8 2003 (Fig. 2). The aRPD depth was calculated as the digitized area divided by the width of the image to provide an average depth across the width of the image.

Statistical Methods

Quantile regression was used to investigate the conditional median or other quantiles of the macroalgal biomass as a function of percent cover using the PROC QUANTREG procedure. Least squares regression was used to quantify the relationship between grain size, sediment % OC and % N using the PROC REG procedure. These analyses were performed using SAS Statistical Software Version 9.3.

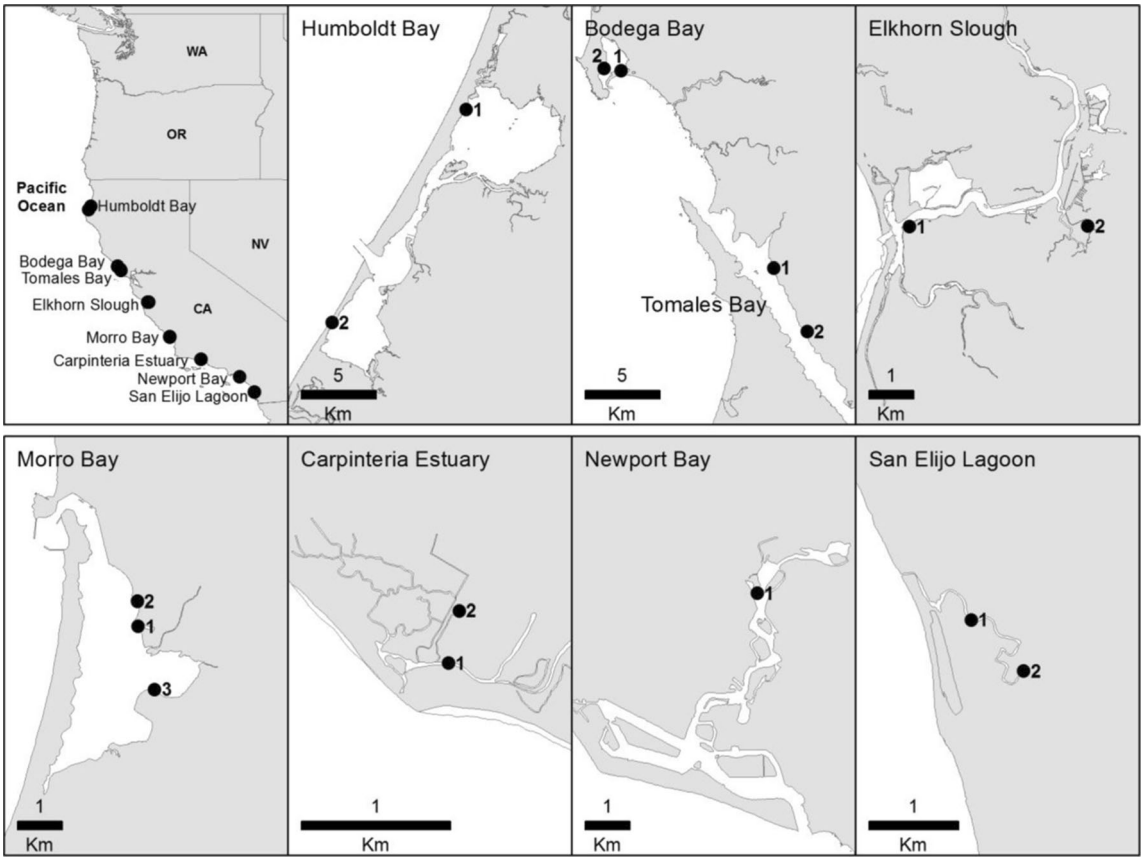

Fig. 1 Map of showing location of estuaries and sampling sites for study

Two types of ecological response thresholds for aRPD were investigated. The first type, a "step" threshold, was evaluated as a statistically significant change in magnitude of aRPD along gradients of sediment % N, sediment % C, and macroalgal dry weight biomass. In this case, the step threshold answers the question "At what level of stressor can you detect an overall reduction in aRPD between reference and impacted classes?" The region along the stress–response curve before

Table 1 Estuary name, locations, class and size, and the latitude and longitudes of sites sampled in the study

Estuary name	Region	Size (km^2)	Site number	Latitude, longitude
Humboldt Bay (HB)	North Coast	66.10	1	N 40°51.019′, W 124°9.559′
			2	N 40°43.067′, W 124°15.500′
Bodega Bay (BB)	North Coast	3.72	1	N 38°18.935′, W 123°2.601′
			2	N 38°18.9931′, W 123°3.401′
Tomales Bay (TB)	North Coast	31.15	1	N 38°11.970′, W 122°55.280′
			2	N 38°9.696′, W 122°53.660′
Elkhorn Slough (ES)	Central Coast	4.17	1	N 36°48.566′, W 121°46.972′
			2	N 36°48.611′, W 121°44.284′
Morro Bay (MB)	Central Coast	10.21	1	N 35°20.7201′, W 120°50.636′
			2	N 35°21.021′, W 120°50.652′
			3	N 35°19.959′, W 120°50.384′
Carpinteria Estuary (CE)	South Coast	0.85	1	N 34°23.900′, W 119°32.081′
			2	N 34°24.057′, W 119°32.041′
Newport Bay (NB)	South Coast	6.7	1	N 33°38.478′, W 117°53.374′
San Elijo Lagoon (SL)	South Coast	2.15	1	N 33°00.679′, W 117°16.443′
			2	N 33°00.358′, W 117°16.076′

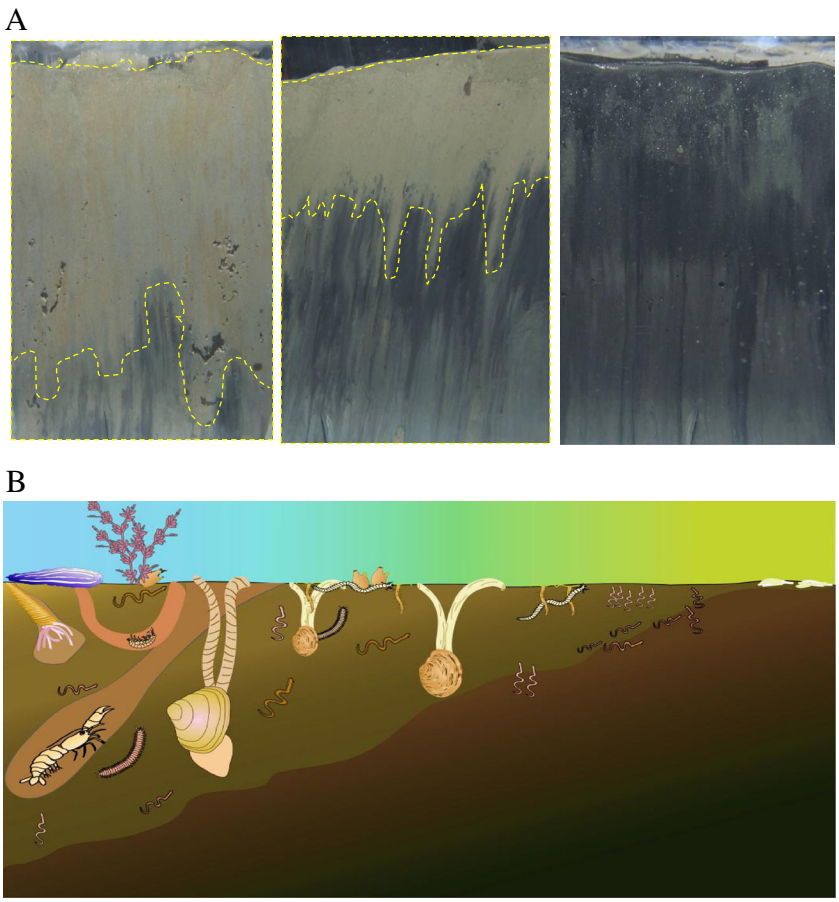

Fig. 2 Example of sediment profile images (**a**) from showing aRDP varying from 8.3, 3.7 and 0 cm (left to right panel, respectively). *Vertical length* of image represents 10 cm in depth. *Dotted line* represents digitized area of aRDP. Images are contrasted against an illustration (**b**) of the Pearson and Rosenberg (1978) conceptual model depicting changes in macrobenthic community structure with increasing organic matter accumulation in the sediment. The model illustrates a gradient of primary condition categories from left to right: non-eutrophic (left side), intermediate eutrophication (middle), and severe eutrophication with anoxic bottom water and azoic sediments (right side of figure). From Gillette and Sutula in Sutula (2011)

the step threshold corresponds to a "reference envelope." The second type, a "slope" threshold, was evaluated as a detectable change in slope of aRPD to each of the three stressors. The slope threshold can be interpreted as the point at which one could expect to see an improvement in benthic condition as stressor levels are reduced, or conversely, the point at which maximum benthic degradation is achieved because the sediments have become anoxic to the surface (Fig. 2). The latter is analogous to an exhaustion threshold based on Cuffney et al.'s (2010) definition.

Step thresholds were analyzed using Classification and Regression Tree (CART) analysis with SYSTAT software (Breiman et al. 1984). A maximum split number of 2 was set, with $p<0.05$ as the stopping criteria. One thousand bootstrapping iterations were run with 10 % replacement to generate confidence intervals for step thresholds. Step thresholds were evaluated both at the plot scale ($n=305$) and at the site scale ($n=16$), the latter using site averages. The former allows a more accurate assessment of the level of stressor associated with an impact because of the variation in stressor levels within sites. However, because macroalgal biomass is typically averaged at the transect- or site-scale, site-level thresholds were also of interest. Potential effects of spatial autocorrelation on results of plot-scale analyses were evaluated using partial Mantel tests of residuals from CART analysis in R with the ECODIST package (Goslee and Urban 2007). Step thresholds were calculated for each dominant algal genus individually at the plot level (*Ulva* spp., *Ceramium* spp., *Gracilaria* spp., and *Lola* spp.) and all algal species together.

Slope thresholds for average and median response were evaluated through piecewise regression analysis using the NONLIN (nonlinear curve fitting) procedure in SYSTAT (Systat Software, Inc., Chicago, IL, USA). Piecewise regression analysis allows evaluation of a segmented linear response with a change in slope at one or more points. To facilitate convergence, models were fit in two stages. First, models were fit with fixed thresholds based on a series of ten potential values chosen at equal intervals along a log10 scale of each stressor variable (sediment N, sediment C, or macroalgal biomass dry weight). The model with the best fit in each series then was used as an initial estimate for the slope break variable in a model fitting procedure in which all three parameters were optimized (y-intercept (b_0), initial slope (b_1), and break), e.g.,

$$\begin{aligned}\text{aRPD} = {} & (\text{Sediment}\,\%\text{N} < \text{break}) * (b_0 + (b_1 * \text{Sediment}\,\%\text{N})) \\ & + (\text{Sediment}\,\%\text{N} \geq \text{break}) * (b_0 + (b_1 * \text{break}))\end{aligned}$$

This model form assumes that aRPD decreases until it reaches a low value and then remains constant with increasing sediment N. Models were fit using both the least-squares minimization and robust regression techniques (based on least absolute deviation). The latter technique is robust to outliers both in the response variable and in covariates (Birkes and Dodge 1993). Final models were evaluated based on Aikake's Information Criterion corrected for small sample size (AICc; Burnham and Anderson 2002). Three alternative models were evaluated — one with no slope, one with a slope but no break point, and one with an initial slope and break point. In general, slope models performed better at the site-averaged rather than plot scale because not all sites had sediment conditions spanning the slope threshold; site-scale also has the advantage that macroalgal biomass is typically reported as a transect-average, so site-averaged thresholds are more relevant for this type of data. In cases where the slope–no slope break models provided the best fit, the x-intercept was calculated as an indicator of the point of adverse effect and confidence intervals were generated in SYSTAT using bootstrap analysis.

Percent cover was not a good indicator of effects on aRPD and thus results for % cover are not shown. At the site scale, only 59–69 % of bootstrap CART trials yielded one or more significant cut point values. Outlier sites (Elkhorn Slough Site 1 and Humboldt Bay Site 2, hereto referred to as ES-1 and HB-2, respectively, with very high macroalgal biomass, low %fines, sediment % OC and % N, were removed from the analysis of step thresholds for biomass because it is suspected that these transects represent high energy sites where it is likely that macroalgae had rafted up and was deposited (Rhoads and Germano 1982).

Results

Range of Conditions Within and Across Estuaries

Taken collectively across all estuaries (Fig. 1), the sites we sampled represented a wide range in condition with respect to sediment bulk characteristics (0.01–22.6 % OC, 0.02–1.57 % N, and 0–96 % fines), aRPD depth (0–17 cm), macroalgal biomass (0–1717 g dw m^{-2}), and macroalgal cover (0–100 %; Table 2). Many sites showed a broad distribution of these properties as well; notable exceptions to this included Elkhorn Slough site 2, which consistently had very low aRPD and very high sediment % OC, % N and macroalgal abundance, and Carpinteria Estuary site 2, which had no macroalgae present during the time of sampling.

Four of eight estuaries (Elkhorn Slough, Morro Bay, Carpinteria Estuary, and San Elijo Lagoon) were completely dominated by *Ulva* spp. (*U.* intestinalis, *U.* expansa, or *U.* lactuca). An additional three were co-dominated by *Ulva* spp. and other species of red (*Gracilaria* spp. in Bodega Bay and Tomales Bay) or green algae (*Lola* spp. in Humboldt Bay). Newport Bay was the only system in which the red algal genus *Ceramium* spp. was found and it completely dominated biomass in this estuary.

Relationships between Macroalgal Biomass and Macroalgal Cover

Across estuaries, algal biomass generally increased with increasing % cover (Supplemental materials, Fig. 1A). Both low and high biomass were possible at high % cover; for example, at >80 % cover, 20 % of plots were below 16 g dw m^{-2} while 20 % of plots were above 93 g dw m^{-2}. At 100 % cover, 60 % of plots exceeded 100 g dw m^{-2}. However, high biomass generally did not occur at low % cover; at <30 % cover, only 5 % of plots exceeded a biomass of 14 g dw m^{-2}.

Relationships among Sediment Percent Organic Carbon, Nitrogen and Grain Size

Across estuaries, sediment % OC and % N were highly positively correlated with % fines ($p<0.0001$ for both correlations); a least squares regression of % fines with the square root of % OC and square root of % N resulted in a linear fit of $R^2=0.53$ and 0.55, respectively. Sediment % OC and % N showed a high degree of covariance ($p<0.0001$, $R^2=0.98$).

Thresholds for Macroalgal Biomass, Sediment % OC, % N Relative to aRPD

Grouping data across estuaries and algal genera, CART analysis allowed us to identify relatively tight step thresholds based on plot-scale data for sediment % N, sediment % OC, and macroalgal biomass; Fig. 3a–c). Similar thresholds were found on site-scale averages for sediment N (0.064 % N) and sediment C (0.70 % C; Fig. 4b,c), but were slightly higher and less certain for site-scale as compared to plot-scale sediment % OC (Figs. 3c and 4c). Although CART analysis identified a step threshold for site-averaged macroalgal biomass (52.6 g dw m^{-2}) it was very diffuse (wide confidence interval), even after the ES-1 and HB-2 outlier site data had been removed (Fig. 4a). Partial Mantel tests showed no evidence of spatial autocorrelation in residuals from CART analyses of the plot data using either sediment % OC or % N ($p>0.05$) and only marginal evidence for spatial autocorrelation of residuals from CART analysis based on macroalgal biomass dry weight ($p=0.05$).

With respect to slope thresholds, the best site-average model fits for aRPD versus sediment % N were those that incorporated both an initial slope term and a break in slope, based on AICc criteria (Table 3; Fig. 5a). Removing outliers

Table 2 Mean and standard deviation (SD) of % OC, % N, aRPD (cm), and macroalgal biomass and cover of 20 plots per estuary site

Estuary	Site no.	aRDP		Sediment % OC (g dw)		Sediment % N (g dw)		Macroalgal biomass (g dw m^{-2})		Macroalgal cover (%)	
		Mean±SD	Range	Mean±SD	Range	Mean±SD	Range	Mean±SD	Range	Mean±SD	Range
Humboldt Bay (HB)	1	3.0±1.5	0.6–7.3	0.5±0.2	0.2–1.0	0.05±0.02	0.03–0.09	85.0±57.8	0.0–235.0	77±35	0–100
	2	3.8±3.4	0.2–10.1	0.2±0.0	0.1–0.3	0.03±0.01	0.02–0.04	226.0±148.1	0.0–507.9	88±30	0–100
Bodega Bay (BB)	1	3.6±2.4	0.2–11.3	0.1±0.0	0.0–0.2	0.02±0.01	0.01–0.03	7.3±14.9	0.0–51.5	17±33	0–100
	2	1.3±1.9	0.1–6.6	0.3±0.1	0.2–0.6	0.06±0.01	0.04–0.09	228.4±407.8	29.2–1,716.9	83±16	56–100
Tomales Bay (TB)	1	7.8±3.5	4.2–17.0	0.3±0.0	0.2–0.4	0.03±0.01	0.02–0.04	5.7±16.1	0.0–74.7	27±32	0–100
	2	7.9±3.6	0.6–12.8	0.4±0.1	0.3–0.5	0.05±0.01	0.03–0.06	3.5±12.1	0.0–54.0	8±23	0–100
Elkhorn Slough (ES)	1	8.7±2.6	1.1–12.2	0.3±0.1	0.2–0.6	0.04±0.01	0.03–0.07	165.9±91.5	0.5–335.5	96±9	67–100
	2	0.6±1.0	0.1–4.1	9.5±4.9	3.8–22.6	0.77±0.31	0.43–1.57	264.5±159.8	4.1–750.0	95±16	33–100
Morro Bay (MB)	1	2.3±3.0	0.0–8.6	0.6±0.2	0.3–0.9	0.08±0.02	0.05–0.12	83.0±33.8	0.0–138.0	98±6	78–100
	2	5.4±1.4	2.1–7.2	0.1±0.0	0.1–0.2	0.02±0.01	0.02–0.03	65.3±125.4	0.0–493.9	47±42	0–100
	3	2.6±2.3	0.0–8.1	0.8±0.4	0.3–1.9	0.12±0.05	0.05–0.28	53.3±30.8	0.0–107.8	83±32	0–100
Carpinteria Estuary (CE)	1	1.0±0.8	0.0–2.9	1.7±0.2	1.3–2.1	0.18±0.03	0.13–0.24	23.5±29.0	0.0–103.2	41±40	0–100
	2	3.1±1.2	1.3–5.6	0.7±0.2	0.4–1.1	0.08±0.03	0.05–0.14	0.0±0.0	0.0–0.0	0±0	0–0
Newport Bay (NB)	1	3.4±2.0	0.7–9.3	0.6±0.1	0.4–0.9	0.07±0.01	0.05–0.10	4.4±7.0	0.0–29.8	17±28	0–100
	2	4.1±2.7	0.7–12.0	0.6±0.1	0.4–0.8	0.07±0.02	0.04–0.12	17.4±21.6	0.0–84.3	41±34	0–100
San Elijo Lagoon (SL)	1	5.3±3.1	0.0–10.4	0.5±0.5	0.2–2.4	0.06±0.04	0.02–0.21	8.0±11.2	0.0–45.9	31±42	0–100
	2	2.7±2.3	0.3–6.5	2.4±0.4	1.7–3.2	0.29±0.05	0.19–0.39	69.9±68.8	0.0–220.0	67±37	0–100

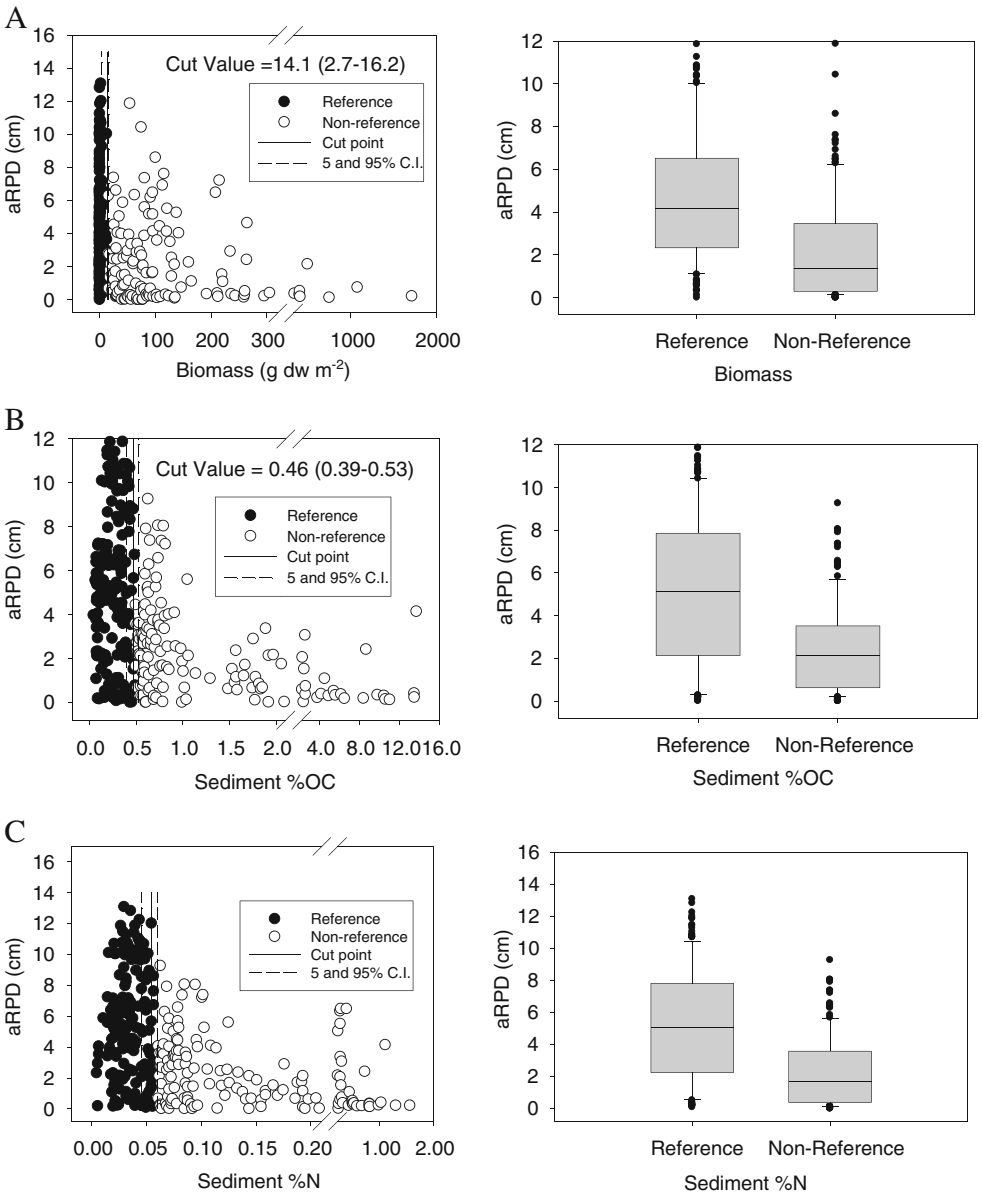

Fig. 3 aRPD as a function of biomass (**a**), sediment % N (**b**) and sediment % C (**c**) with *X* axis delineating low and high aRPD groups as defined by bootstrapped CART analysis for plot level data. Mean threshold is shown as the *solid vertical line* with 5th and 95th percentiles as dashed lines. *Box plots* (*right-hand graphic*) for two groups are next to scatter plot (*left-hand graphic*). Biomass thresholds shown reflect elimination of ES-1 and HB-2 outliers

ES-1 and HB-2 improved fits for % N, % OC and biomass models. The slope threshold was similar between least-squares and robust regression results, at ~0.11 % and ~0.14 % N, respectively, approximately double that of the step thresholds presented above. The best site-average model fits for aRPD versus sediment % OC did not include the models with a slope change, although relative likelihoods were still relatively high for the latter, and the robust regression model fit with a slope break parameter was better than the model with only intercept and slope terms. The least squares and robust regression slope thresholds were 1.08 % and 1.22 % OC, respectively, again, higher than for the corresponding step threshold (Fig. 5b). The best site-average model fits for aRPD versus macroalgal biomass did not include the models with a slope change; a "no break" slope model was more significant than one with a slope break, regardless of whether ES-1 and HB-2 were excluded (Table 3). After removing these outliers, the least squares model median *X*-intercept (representing the macroalgal biomass at which aRPD approaches zero) was 319 g dw m^{-2}, with 5th and 95th percentiles ranging from 175 to 358 g m^{-2} (Table 4). The 5th percentile (175 g dw m^{-2}) of this *X* intercept provides a more conservative estimate of an effects threshold than the 50th or 95th percentile. The robust model gave results similar to the least squares model results for the *X* intercept (189–358 g m^{-2}). In this case, the effect of trailing data points at near zero aRPD values with increasing biomass causes an increase in the median value of the *X* intercept and a widening of this confidence interval. Including these outliers caused a further widening of confidence intervals.

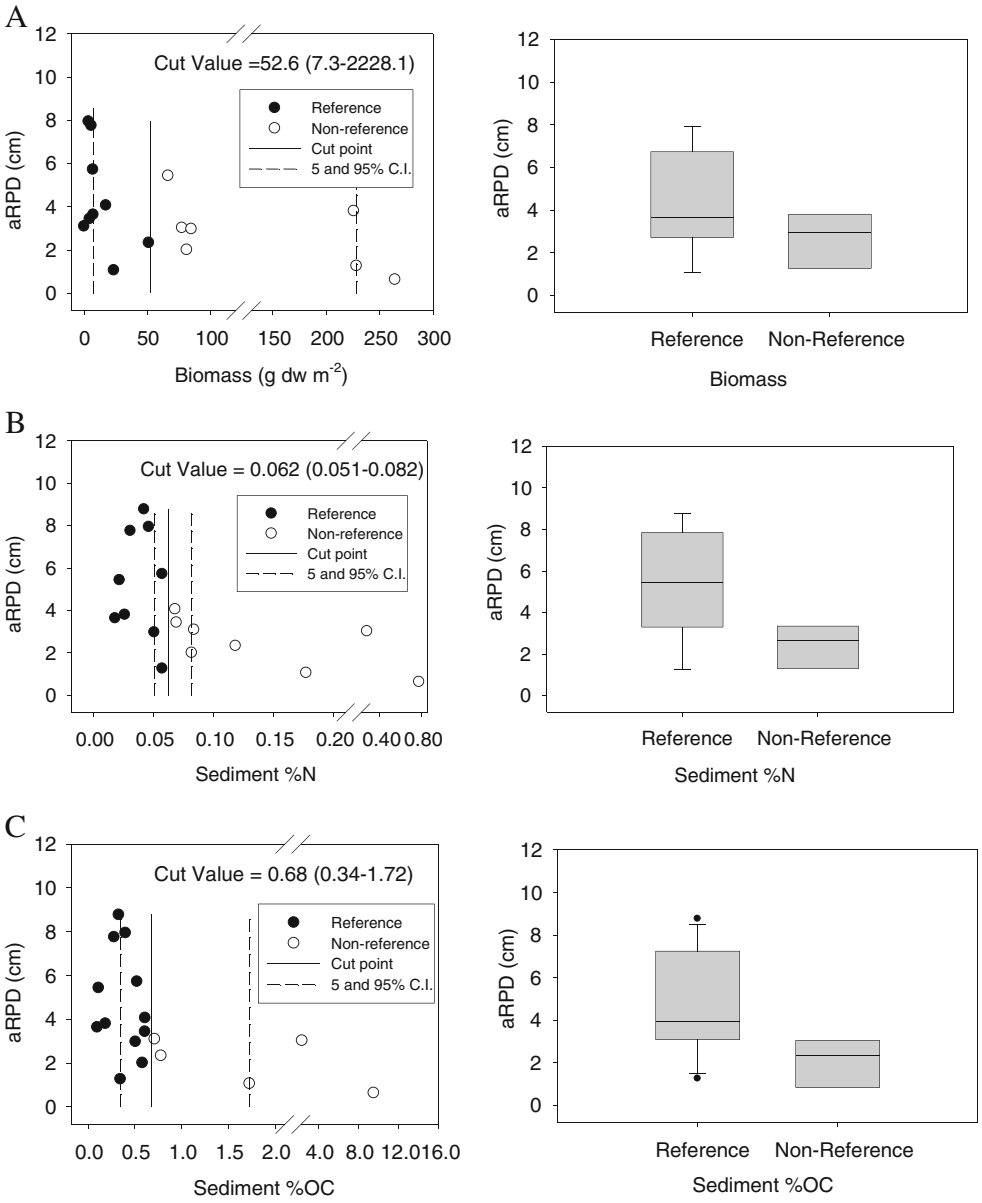

Fig. 4 aRPD as a function of biomass (**a**), sediment % N (**b**) and sediment % OC (**c**) with *X* axis delineating low and high aRPD groups as defined by bootstrapped CART analysis for site-averaged data. Mean threshold is shown as the *solid vertical line* with 5th and 95th percentiles as *dashed lines*. *Box plots* (*right-hand graphic*) for two groups are next to scatter plot (*left-hand graphic*). Biomass thresholds shown reflect elimination of ES-1 and HB-2 outlier

Analysis of data at the algal genus level gave step thresholds for % C and % N that were relatively consistent with those identified for data grouped across algal genera (0.18–0.63 % C and 0.03–0.07 % N; Table 5). For biomass, there was more variability. Step thresholds for *Ulva* spp., *Ceramium* spp. and *Gracilaria* spp. ranged from a low of 9.4 to 46.1 g dw m^{-2}, while the threshold for *Lola* spp. was substantially higher (261 g m^{-2}). The step threshold for biomass grouping by algal genera (7.2 g m^{-2}) was lower than that which excluded only *Lola* spp. (13.1 g m^{-2}), though the confidence intervals were virtually identical (2.7–16.2 g m^{-2}). Interestingly, the comparisons of % N and % C thresholds for plot-level data with and without *Lola* spp. were not significantly different, suggesting that plots dominated by *Lola* spp. did not have a strong feedback loop with sediments. Mean sediment % OC at *Lola* spp.-dominated sites was low (0.18± 0.04 % OC), despite high biomass (251±138 g dw m^{-2}). In contrast, plots with high *Ulva* spp. biomass (>100 g m^{-2}) were associated with very high sediment % OC (>1 % OC; Fig. 6).

Discussion

Our study of aRPD in the intertidal flats of eight California estuaries identified two types of statistically defined thresholds for macroalgal biomass, sediment % C, and % N as stressors to benthic habitat: (1) a step threshold which identifies the range in concentration at which there is a detectable overall reduction in aRPD between reference (reference

Table 3 Piecewise regression analysis of site-averaged aRPD response as a function of sediment % N, sediment % C, and macroalgal biomass

Fit method	Predictor	Parameter Estimates (Wald 95 % CI)			*n*	Residual SS	Full model	No break	No slope	Relative likelihood of sign. break	Relative likelihood of sign. slope
		Break	*y*-Intercept	Initial slope			AICc	AICc	AICc		
Least squares	% N	0.11 (0.017 to 0.21)	6.7 (3.8 to 10.3)	−45.5 (−103.0 to 12.1)	17	58.2	80.5	**77.1**	82.3	0.19	**13.38**
Robust regression	% N	0.14	6.3	−37.4	17	60.0	81.0	**77.8**	83.1	0.20	**14.21**
Least squares[a]	% N	0.11 (0.029 to 0.18)	7.4 (4.0 to 1.0)	−54.26 (−116.1 to 0.6)	16	54.9	**76.8**	77.8	78.9	**1.71**	**1.67**
Robust regression[a]	% N	0.14	6.2	−37.7	16	58.6	**77.8**	78.9	79.6	**1.73**	**1.38**
Least squares	% C	1.17 (−0.17 to 2.51	6.1 (3.3 to 9.0)	−3.9 (−9.8 to 1.9)	17	65.2	82.4	**81.7**	82.3	0.71	**1.35**
Robust regression	% C	1.20	5.9	−4.0	17	67.2	**82.9**	83.1	83.1	**1.07**	**1.00**
Least squares[a]	% C	1.08 (−0.011 to 2.16)	6.5 (3.4 to 9.8)	−4.6 (−11.1 to 1.8)	16	62.9	78.9	**78.5**	78.9	0.82	**1.18**
Robust regression[a]	% C	1.22	5.8	−3.9	16	66.5	79.8	80.3	**79.6**	**1.24**	0.70
Least squares	Biomass	23.6 (−219.5 to 266.6)	5.5 (2.6 to 8.7)	−0.09 (−0.4 to 0.2)	17	89.4	87.8	83.6	**82.3**	0.12	0.53
Robust regression	Biomass	96.6	3.8	−0.01	17	81.4	86.2	86.4	**83.1**	**1.09**	0.19
Least squares[a]	Biomass	23.58 (−11.4 to 58.6)	5.8 (3.2 to 8.4)	−0.1 (−0.5 to 0.2)	15	44.4	70.9	**67.5**	70.7	0.19	**5.04**
Robust regression[a]	Biomass	23.58	6.3	−0.2	15	44.8	71.0	**69.8**	71.6	0.54	**2.48**

Models with and without break point and with and without slope are compared using AIC criterion corrected for small sample size (AICc). Best (lowest) AICc is shown in *bold*. Relative likelihood of a significant slope or of having a break in slope are shown in *bold* for values greater than 1. Results shown for models with and without ES-1 and HS-2 outliers removed

[a] Outlier ES-1 and HS-2 removed

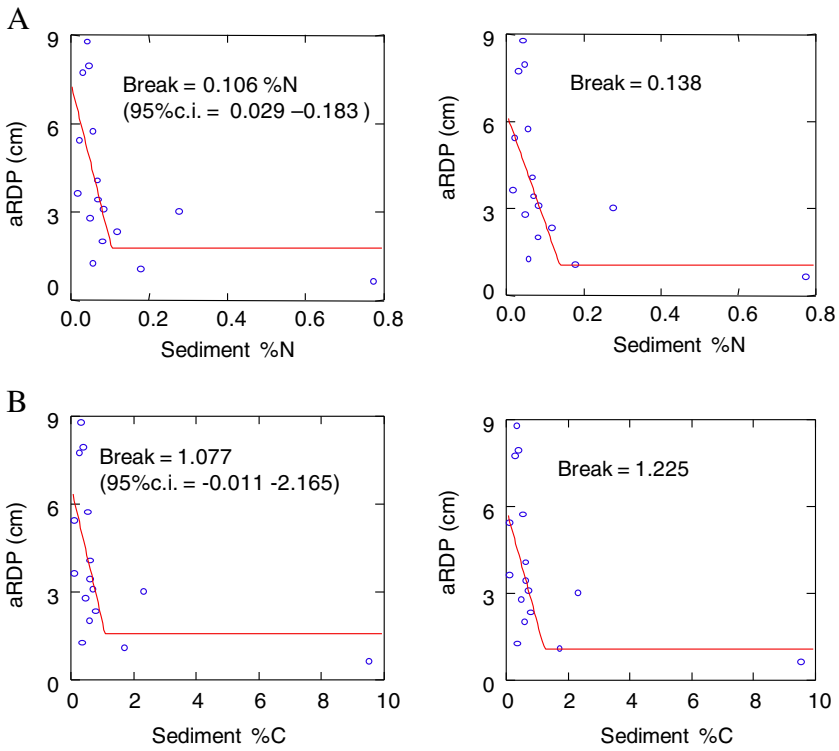

Fig. 5 Piecewise regression analysis of relationship between aRPD (cm) and site-average sediment % N (**a**) and sediment % C by least-squares (*left side* of panel) and robust regression (*right side* of panel)

envelope) and non-reference sites and (2) a slope break threshold, which is the point at which maximum benthic degradation is achieved because anoxic sediments extend to the sediment surface. Ecologically, this slope break threshold is equivalent to an "exhaustion threshold" (Cuffney et al. 2010). Controls on aRPD formation are complex, responding to a variety of driving factors including oxygen concentrations, bioturbation, sediment % OC, carbonate and iron content, physical energy, and a host of other physical and sediment attributes — all of which vary temporally and spatially within estuarine sediments (Conley et al. 2009; Teal et al. 2010; Viaroli et al. 2010). In our study of estuarine intertidal flats, aRPD was highly variable, reflective of a broad range of conditions captured among these eight estuaries. However the slope break (sediment % OC and % N) or 5th percentile of the *X* intercept (macroalgae) in the no-slope-break models represents an exhaustion threshold in organic matter accumulation that appears to override other factors controlling aRPD, driving it to near zero levels. This collapse in aRPD translates to reduced habitat volume and quality for benthic infauna and alteration in their community structure (Pearson and Rosenberg 1978; Nilsson and Rosenberg 1997; Rosenberg et al. 2003). These effects have been linked to reduced availability of forage for fish, birds and invertebrates (Raffaelli

Table 4 *X*-intercept corresponding to simple linear model is shown based on bootstrap analysis (n=1,000, median, 95 % confidence interval), given for no-break models (see Table 4 above)

Fit method	Predictor	*Y*-intercept	Slope	*X*-intercept	*X*-intercept parameter estimates (bootstrap 95 % CI)		
					Median	5th	95th
Least squares	Sediment % N	4.7	−6.36	0.74	0.73	0.18	0.87
Robust regression	Sediment % N	3.9	−4.23	0.92	0.91	0.20	1.24
Least squares	Sediment % C	3.8	−0.33	11.4	9.39	1.87	10.96
Least squares	Biomass	4.6	−0.0085	537.8	445.7	0.0	1,931.4
Robust regression	Biomass	3.9	−0.012	336.8	323.6	0.0	2,177.6
Least squares[a]	Biomass	4.5	−0.013	362.5	318.6	175.8	358.8
Robust regression[a]	Biomass	3.9	−0.011	339.1	318.0	189.4	358.7

[a] Outlier ES-1 and HS-2 removed

Table 5 Mean (5–95th percentile) cut values for step thresholds, based on results of aRPD as a function of biomass, sediment % N and sediment % C as defined by bootstrapped CART analysis for plot level data

Parameter	Dominant algae group	Mean (5th–95th percentile) of cut value	Model fit (R^2)
Macroalgal Biomass (g dw m^{-2})	*Ulva* spp.	28.9 (2.1–296.0)	0.12
	Ceremium spp.	46.1 (3.3–85.5)	0.38
	Gracilaria spp.	9.1 (2.0–15.2)	0.18
	Lola spp.	261.3 (156.1–443.5)	0.28
	All	7.2 (2.7–15.2)	0.09
Sediment % N	*Ulva* spp.	0.06 (0.05–0.09)	0.35
	Ceremium spp.	0.05 (0.04–0.06)	0.36
	Gracilaria spp.	0.07 (0.05–0.10)	0.13
	Lola spp.	0.03 (0.02–0.03)	0.29
	All	0.06 (0.05–0.07)	0.22
Sediment % OC	*Ulva* spp.	0.44 (0.40–0.49)	0.36
	Ceremium spp.	0.34 (0.29–0.43)	0.19
	Gracilaria spp.	0.63 (0.47–0.79)	0.13
	Lola spp.	0.18 (0.16–0.21)	0.26
	All	0.49 (0.39–0.78)	0.19

et al. 1989, 1991; Bolam et al. 2000). Thus the ranges associated with "reference" and near zero aRPD represent bookends of a gradient of increasing organic matter loading along which increasing adverse effects can be documented. Site-specific differences in response to stressors among or within estuaries and other sources of variation produce a widening of the gap between as well as the confidence intervals around these "bookends" of stress levels.

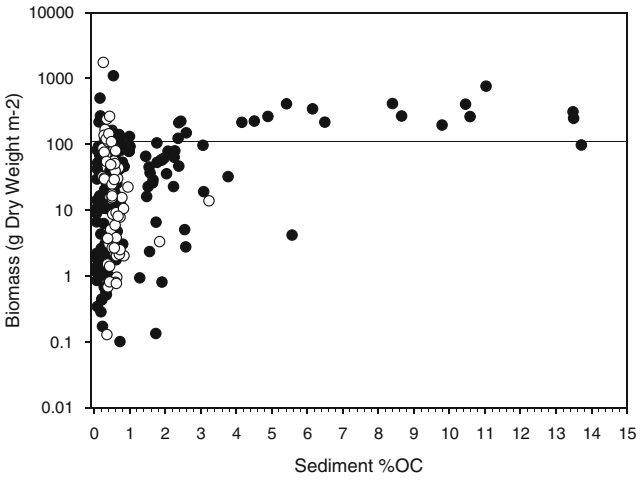

Fig. 6 Relationship between sediment % OC and macroalgal biomass. Color of symbol indicates algal genus, where green algae (*Ulva* spp.) is marked by *black circle* and red algae (*Ceremium* spp. and *Gracilaria* spp.) by *white circle*

We found that biomass of 3–15 g dw m^{-2} represented a statistically defined reference envelope, or range of macroalgal abundance at which no detectable effect on aRPD was evident in these eight California estuaries. This reference envelope was identified through detection of step thresholds, the point at which overall reduction occurs in aRPD between reference and impacted classes. We found no previous studies that have reported reference levels of macroalgae in intertidal flats. However, the proposed macroalgal assessment framework for the European Union Water Framework Directive (EU WFD; Scanlan et al. 2007), which was created based on expert best professional judgment, categorized estuaries with 0–100 g ww m^{-2} (~0–10 g dw m^{-2}) as in high ecological condition. This expert-defined "reference envelope" agrees well with our statistically derived range of 3–15 g dw m^{-2} (Scanlan et al. 2007). This reference envelope, representing the characteristics of "least disturbed" sites with respect to aRPD, can be distinguished from benchmarks of "no observed effects levels," in which some effects of the stressor may be apparent, but not adverse effects. A field experiment by Cardoso et al. (2004) found a positive effect on invertebrate diversity and abundance at approximately 30 g dw m^{-2} (300 g ww m^{-2}; Cardoso et al. 2004), though the treatment was a single rather than continuous application.

In contrast to the defined reference envelope, a macroalgal biomass of 175 g dw m^{-2} appears to be an exhaustion threshold where aRPD depth approaches zero, corresponding to strong adverse effects to benthic habitat quality. A literature survey of field experiments reporting effects of macroalgal biomass on benthic infaunal community structure generally supports these findings, with adverse effects reported at ranges from 110 to 863 g dw m^{-2} (840–6,000 g ww m^{-2}; Table 6). Most of these studies were based on a single treatment level and a one-time application of algae; therefore the utility of many of these studies to identify benchmarks of adverse effects associated with macroalgae biomass is limited. However, three studies are of particular interest. Green et al. (2013) conducted experiments at four sites in two California estuaries with five treatment levels of macroalgal biomass, controlling for duration. They documented significant adverse effects to benthic infaunal diversity at 110–120 g dw m^{-2} (840–940 g ww m^{-2}); at this level, total macrofaunal abundance decreased by at least 67 % and species richness declined at least 19 % within 2 weeks at three of the four sites in the two estuaries. At this benchmark, surface deposit feeders significantly declined, a functional group important as a forage for fish and birds (Posey et al. 2002). Similarly, Bona (2006) found an adverse effect level of 700 g ww m^{-2} to (90 g dw m^{-2}) using SPI to identify thresholds of macroalgal biomass associated with a significant decline in large filter feeders. We interpret the thresholds identified by these two studies to represent a lowest observed effect level, representing intermediate adverse effects

Table 6 Summary of observed effects of macroalgal abundance on infauna and resident epifauna on intertidal flats (from Sutula 2011)

Location	Source	Treatment level/observed abundance	Duration	Observed	Comments
Baltic Sea	Norkko and Bonsdorff 1996	2 kg ww m^{-2}	34 days	Reduced abundance of most macrobenthic invertebrates but not all	~280 g dw m^{-2}, Single treatment level — single algal application
Australia	Cummins et al. 2004	4.5 kg ww m^{-2}	12 weeks	Reduced macrobenthos species abundance	~640 g dw m^{-2}, Single treatment level — single algal application
Portugal	Cardoso et al. (2004)	0.3 kg ww m^{-2} no effect 3 kg ww m^{-2} adverse effect	4 weeks	Reduced macrobenthos species abundance species specific response	~30 g dw m^{-2}; Multi treatment levels — single algal application
California	Green (2010)	0.5 cm (60 g dw m^{-2}) no adverse effect after 8 weeks; 1.5 cm (186 g dw m^{-2}) adverse effect after 4 weeks; 3.0 cm (416 g dw m^{-1}) adverse effect after 2 weeks	2–8 weeks	Increased biomass reduced surface deposit feeders and increased subsurface deposit feeders	Multi treatment levels — maintained algal treatment level biweekly
Scotland	Hull (1987)	3 kg ww m^{-2} adverse effects were species specific	22 weeks	After 10 weeks some surface deposit feeders decreased while some subsurface feeders increased. After 22 weeks patterns similar	~420 g dw m^{-2}; multi treatment levels — single algal application
Scotland	Raffaelli (2000)	No biomass treatment after 10 weeks increase is species specific. 3 kg ww m^{-2} after 10 weeks adverse effects are species specific. Equivalent abundances of both species in all treatments after 22 weeks	22 weeks	High abundances result in increase of subsurface deposit feeders, decrease in surface deposit feeders after 10 weeks.	~420 g dw m^{-2}; multi treatment levels— single algal application
Sweden	Osterling and Pihl (2001)	1.2 kg ww m^{-2} adverse effect on all taxa after 21 days Adverse effect on some taxa after 36 days	36 days	Initially all macrofauna were negatively affected by macroalgae. After 36 days subsurface detritivores and carnivores positively affected	~160 g dw m^{-2}; single treatment level — single algal application
California	Everett (1991)	~6 kg ww m^{-2} adverse effects after 2 and 6 months	6 months	Clams and shrimp abundance increased in plots where macroalgae was removed	~863 g dw m^{-2}; removal experiment
Scotland	Bolam et al. (2000)	~1 kg ww m^{-2} species specific effects after 6 and 20 weeks	20 weeks	Surface deposit feeders negatively affected, subsurface feeders positively affected after 6 weeks effects persisted through 20 weeks	~131 g dw m^{-2}; single treatment level — single algal application
England	Jones and Pinn (2006)	Adverse effects >70 % cover	Not recorded	Species diversity declined when % cover increased from 5 % to 70 % in 1 month	Correlative field study. Low cover did not always=high diversity
Sweden	Pihl et al. 1995	Some negative effects with 1 % cover, greatest effects >30 % cover	Not recorded	Crabs negatively affected by moderate and high percent cover	Correlative field study. One-day sampling events
Baltic Sea	Lauringson and Kotta (2006)	No clear relationship with mat depth and infaunal abundance	Not recorded	Herbivores more prominent within mats, detritivores more prominent in sediment	Correlative field study. Subtidal
Italy	Bona (2006)	0.7 kg ww m^{-2} and >70 % cover	Not recorded	Loss of Stage III benthic colonization by filter feeders	~90 g dw m^{-2}; use SPI camera for correlative field study
California	Green et al. (in press)	Identified 110–120 g dw m^{-2} at 4 weeks as benchmark for adverse effects.	10 weeks	Reduced diversity and abundance of surface deposit feeders	Manipulative field experiment with 5 treatment levels and biweekly monitoring of duration

to benthic community structure. At higher abundances, effects on benthic habitat quality are more significant, including sharp declines in abundance of infauna, and the absence of an aRPD, coincident with the production of high pore water sulfide and ammonium concentrations. For example, Green (2010) demonstrated that macroalgal mats of 190 g dw m^{-2} (1,373 g ww m^{-2}) produced pore water sulfide in surficial sediments (0–4 cm) at concentrations known to be toxic to infauna after 8 weeks. This work agrees with our observed severe effects threshold of 175 g dw m^{-2} associated with near zero aRPD.

Unlike previous studies (Pihl et al. 1995; Bona 2006; Jones and Pinn 2006), our study did not find a strong relationship between macroalgal % cover and aRPD. In the previous two studies, no documentation of biomass was made, only cover, so it is not possible to understand how cover related to organic matter loading (biomass). In Bona (2006), cover greater than 70 % was generally associated with absence of large filter feeders. Furthermore, during the preliminary growth phase, macroalgae will typically exhibit a very thin layer of biomass at high cover. Our data as well as other studies have demonstrated that it is possible to document high % cover with little measureable biomass (McLaughlin et al. 2013). Cover is an important variable in estimating the spatial patchiness or extent of an effect (Scanlan et al. 2007). Our study found that high biomass generally did not occur at <30 % cover. Thus percent cover has the potential to be used as a screening indicator to identify areas of potential risk to macroalgal blooms, because measurement of biomass is more labor intensive and costly than measurement of cover.

As with macroalgae, our study defined two types of thresholds for sediment % OC and % N in intertidal flats: 1) exhaustion threshold associated with aRPD approaching near zero and 2) a reference envelope of % OC and % N. Our exhaustion threshold for ecological effects (1.1–1.2 % OC) is lower than in other previously published work in this field, much of which is based on empirical work in subtidal areas. Thresholds or tipping points in % OC leading to adverse effects to benthic invertebrates have been reported at: 2–3 % (Diaz et al. 2008, in Boston Harbor); 2.8 % (Magni et al. 2009, in Mediterranean lagoons); 3.5 % (Hyland et al. 2005, in seven coastal regions of the world). These authors developed useful thresholds for screening over broad coastal areas, but did not quantify sources of variability related to the thresholds. In contrast, Pelletier et al. (2010) used a large data set to evaluate % OC thresholds linked to adverse effects on benthic invertebrates, and quantified variability due to sediment grain size and region. Sediment designated as "enriched" were more likely to have reduced water column dissolved oxygen and adverse effects on benthic invertebrates. This approach provides a more appropriate comparison to our dataset, because % OC varies as a function of grain size. The median grain size distribution in our study for plot level data was 16 % fines, with a 90th percentile of 45 % fines. For grain sizes of <45 % fine, Pelletier et al. (2010) predicted subtidal impairment and enrichment thresholds at % OC values above 1–1.5 % OC for the three Atlantic Coast regions, agreeing well with the exhaustion thresholds of 1.1–1.2 % OC found in our study. Because low oxygen is one of the primary faunal stressors associated with high % OC (Hyland et al. 2005) and the intertidal zone is re-oxygenated on a daily basis, we might expect macrofauna to remain healthy at higher levels of % OC than would those in subtidal habitats (Magni 2003). However, our data do not provide evidence for a difference in these thresholds for sediment organic matter along this intertidal–subtidal continuum.

Pelletier et al. (2010) also defined a reference envelope of % OC at 0.2–0.9 % over our range of 0–45 % fines, values that also agree well with the 0.2–0.7%OC reference transition range identified in our study. In addition to grain size, further sources of variability in empirical relationships between % OC and benthic fauna include the quality and form of organic carbon (Pusceddu et al. 2009), dissolved oxygen, toxicants and nutrients (Hyland et al. 2005). However, Pelletier et al. (2010) accounted for many of these other variables and found that grain size accounted for 65.6–85.5 % of the variation in % OC. This suggests that many of the subtidal studies reporting higher thresholds of % OC for reference (<1 % OC; Hyland et al. 2005) and adverse effects may have been conducted in muddier sediments than we saw in our mostly sandy intertidal setting. Like sediment % OC, % N appeared to exhibit a strong tipping point with respect to aRPD. This is not surprising, given that sediment % N was strongly correlated with % OC. A review of literature shows no studies that provide thresholds specifically for sediment % N; all work has focused on % OC (e.g., Hyland et al. 2005).

It was noteworthy that thresholds associated with aRPD for both % N and % OC were tighter than for macroalgal biomass. This is likely due to the fact that aRPD is directly driven by the introduction of organic matter that increases oxygen demand and stimulates sediment diagenesis, thereby shallowing the aRPD; the effect of macroalgae on aRPD is an indirect effect of feedback loops involving macroalgae and the biogeochemistry of sediment organic matter. Live macroalgae takes nitrogen up from the water and sediment pore waters at a high rate, while releasing labile organic carbon and nitrogen as exudates (Valiela et al. 1997; Fong and Zedler 2000; Fong et al. 2004). However, when macroalgae decay after senescence or shading, they release even more bioavailable organic nitrogen and labile carbon; aRPD has been observed to change suddenly during the oxic–anoxic transition that occurs during the collapse of macroalgal blooms (Viaroli et al. 2010). Thus, macroalgal blooms during growth phases draw down pore water N and during decay phase can enrich sediment % OC and % N in surficial sediments. Sediments with high organic matter content are often associated with chronic macroalgal blooms (Kamer et al. 2004); high macroalgal biomass was

present under a range of % N, but above 0.3 % N, macroalgal biomass was consistently high (>100 g dw m^{-2}). This relationship is reflective of strong feedback between macroalgae and sediment biogeochemical processing. Plots from ES-1 and HB-2, identified and removed as outliers because of consistently high algal biomass, high aRPD and very low % OC and % N, were sites characterized by high hydrodynamic energy that likely led to transient rafting of macroalgal mats into the site. This suggests an important consideration: the use of macroalgal biomass as an indicator of eutrophication: high biomass in the absence of low aRPD, high sediment % OC or % N may indicate temporary rafting rather than an in situ bloom event. If so, evaluation of sediment organic matter content would be a useful line of additional evidence in assessing eutrophication.

Our work presents a significant step forward in quantifying ranges of reference and severe adverse effects associated with macroalgal blooms on intertidal flats, thereby increasing the confidence in use of this indicator for eutrophication assessment and establishment of nutrient-related water quality goals. The inclusion of eight estuaries (representing a range in geoform, tidal forcing, and rainfall in a Mediterranean climate) expands our understanding of uncertainty in applying thresholds from earlier work conducted in single estuaries. Further, our thresholds were selected through statistical analyses, rather than through visual interpretation of the data; confidence intervals in our estimates provide a measure of variability in response across systems. Not all sources of variability were explored in our study. For example, it is reasonable to expect that thresholds of adverse effects as well as reference transition ranges may differ by macroalgal genus. The C/N ratio of biomass, surface area to biomass ratio and growth form (filamentous, sheet-like, etc.) could also be expected to influence the lability of carbon loading to sediments (de los Santos et al. 2009). Because of the lack of sufficient range and sample size at the genus level, we aggregated the data to identify adverse effect levels. The adverse effects ranges identified are most applicable to *Ulva* spp., the genus that dominated our data set at high biomass. Lack of information on the duration of macroalgal blooms, the stage of the blooms (growth or senescence), and the longevity of mats at a particular site are other sources of variability important to threshold identification. For this reason, we see our study as a complement to field experiments in which biomass and duration were tightly controlled (Green et al. 2013). Application of these thresholds in a management context must consider these uncertainties; confidence in their application will increase in circumstances where macroalgal blooms are documented to persist over long period of time (duration) or greater spatial extent (McLaughlin et al. 2013).

Use of macroalgal indicators in regional and national assessments of estuarine eutrophication has previously been hampered by the lack of quantitative data on thresholds (McLaughlin et al. 2013; Bricker et al. 2007). This study statistically defined a reference envelope and exhaustion thresholds for the effects of macroalgae and sediment organic matter on benthic habitat quality, providing data that will help refine the diagnostic frameworks with which these assessments are made (Bricker et al. 2003; Scanlan et al. 2007; Zaldivar et al. 2008; Borja et al. 2011).

Acknowledgments Funding for this study was provided through a contract with the California State Water Resources Control Board (07-110-250-1). This study would not have been possible without the hard work and dedication of students and staff from UCLA and SCCWRP, in particular, Courtney Neumann, who performed all of the digital imaging analysis of the SPI photographs, and Caitlin Fong, Sarah Bittick and Greg Lyon, who led field work. The authors also wish to express their gratitude to Becky Schaffner for assistance with map preparation.

References

Birkes, D., and Y. Dodge. 1993. *Alternative methods of regression*. New York: John Wiley & Sons.

Bolam, S.G., T.F. Fernandes, P. Read, and D. Raffaelli. 2000. Effects of macroalgal mats on intertidal sandflats: An experimental study. *Journal of Experimental Marine Biology and Ecology* 249: 123–137.

Bona, F. 2006. Effect of seaweed proliferation on benthic habitat quality assessed by sediment profile imaging. *Journal of Marine Systems* 62: 164–172.

Borja, A., A. Basset, S. Bricker, J.-C. Dauvin, M. Elliott, T. Harrison, J.-C. Marques, S.B. Weisberg, and R. West. 2011. Classifying ecological quality and integrity of estuaries. In *Treatise on estuarine and coastal science*, ed. E. Wolanski and D.S. McLusky, 125–162. Waltham: Academic Press.

Breiman, L., J.H. Friedman, R.I. Olshen, and C.I. Stone. 1984. *Classification and regression trees*. Belmont: Wadsworth.

Bricker, S.B., J.G. Ferreira, and T. Simas. 2003. An integrated methodology for assessment of estuarine trophic status. *Ecological Modelling* 169: 39–60.

Bricker, S.B., B. Longstaf, W. Dennison, A. Jones, K. Boicourt, C. Wicks, and J. Woerner. 2008. Effects of nutrient enrichment in the nation's estuaries: A decade of change. *Harmful Algae* 8: 21–32.

Burnham, K.P., and D.R. Anderson. 2002. *Model selection and multimodel inference: A practical information—theoretic approach*, 2nd ed. New York: Springer-Verlag.

Cardoso, P.G., M.A. Pardal, D. Raffaelli, A. Baeta, and J.C. Marques. 2004. Macroinvertebrate response to different species of macroalgal mats and the role of disturbance history. *Journal of Experimental Marine Biology and Ecology* 308: 207–220.

Cicchetti, G., J.S. Latimer, S.A. Rego, W.G. Nelson, B.J. Bergen, and L.L. Coiro. 2006. Relationships between near-bottom dissolved oxygen and sediment profile camera measures. *Journal of Marine Systems* 62: 124–141.

Conley, D.J., J. Carstensen, R. Vaquer-Sunyer, and C.M. Duarte. 2009. Ecosystem thresholds with hypoxia. *Hydrobiologia* 629: 21–29.

Cuffney, T.F., R.A. Brightbill, J.T. May, and I.R. Waite. 2010. Responses of benthic macroinvertebrates to environmental changes associated with urbanization in nine metropolitan areas. *Ecological Applications* 20: 1384–1401.

Cummins, S.P., D.E. Roberts, and K.D. Zimmerman. 2004. Effects of the green macroalga *Enteromorpha intestinalis* on macrobenthic and

seagrass assemblages in a shallow coastal estuary. *Marine Ecology-Progress Series* 266: 77–87.

Dauer, D.M., C.A. Maybury, and R.M. Ewing. 1981. Feeding behavior and general ecology of several spionid polychaetes from the Chesapeake Bay. *Journal of Experimental Marine Biology and Ecology* 54: 21–38.

de los Santos, C.B., J.L. Pérez-Lloréns, and J.J. Vergara. 2009. Photosynthesis and growth in macroalgae: linking functional-form and power-scaling approaches. *Marine Ecology Progress Series* 377: 113–122.

Diaz, R.J., R.J. Neubauer, L.C. Schaffner, L. Pihl, and S.P. Baden. 1992. Continuous monitoring of dissolved oxygen in an estuary experiencing periodic hypoxia and the effect of hypoxia on macrobenthos and fish. *Science of the Total Environment* Supplement 1992: 1055–1068.

Diaz, R.J., D.C. Rhoads, J.A. Blake, R.K. Kropp, and K.E. Keay. 2008. Long-term trends of benthic habitats related to reduction in wastewater discharge to Boston Harbor. *Estuaries and Coasts* 31: 1184–1197.

Ferren, W., P. Fiedler, R.B. Leidy, K. Lafferty, and L.K. Mertes. 1996. Classification and description of wetlands of the central and southern California coast and coastal wetlands. *California Botanical Society* 43: 125–182.

Fong, P. 2008. Macroalgal dominated ecosystems. In *Nitrogen in the marine environment*, ed. D.G. Capone, D.A. Bronk, M.R. Mulholland, and E.J. Carpenter, 918–961. New York: Springer.

Fong, P., and J.B. Zedler. 2000. Sources, sinks, and fluxes of nutrients (N+P) in a small highly modified urban estuary in southern California. *Urban Ecosystems* 4: 125–144.

Fong, P., J. Fong, and C. Fon. 2004. Growth, nutrient storage, and release of dissolved organic nitrogen by *Enteromorpha intestinalis* in response to pulses of nitrogen and phosphorus. *Aquatic Botany* 78: 83–95.

Giordani, G., R. Azzoni, M. Bartoli, and P. Viaroli. 1997. Seasonal variations of sulfate reduction rates, sulphur pools and iron availability in the sediment of a dystrophic lagoon (Sacca Di Goro, Italy). *Water, Air, & Soil Pollution* 99: 363–371.

Goslee, S.C., and D.L. Urban. 2007. The ecodist package for dissimilarity-based analysis of ecological data. *Journal of Statistical Software* 22: 1–19.

Green, L. 2010. Macroalgal mats control trophic structure and shorebird foraging behavior in a southern California Estuary. PhD dissertation, University of California Department of Biology and Evolutionary Ecology, UCLA, Los Angeles.

Green, L., P. Fong, and M. Sutula. 2013. Identification of the benchmark of adverse effects by bloom forming macroalgae on macrobenthic faunal abundance, diversity and community composition. *Ecological Applications*. doi:10.1890/13-0524.1.

Groffman, P.M., J.S. Baron, T. Blett, A.J. Gold, I. Goodman, L.H. Gunderson, B.M. Levinson, M.A. Palmer, H.W. Paerl, G.D. Peterson, N.L. Poff, D.W. Rejeski, J.F. Reynolds, M.G. Turner, K.C. Weathers, and J. Wiens. 2006. Ecological thresholds: The key to successful environmental management or an important concept with no practical application? *Ecosystems* 9: 1–13.

Hentschel, B. 1996. Ontogenic changes in particle-size selection by deposit-feeding spionid polychaetes: The influences of palp size on particle contact. *Journal of Experimental Marine Biology and Ecology* 206: 1–24.

Hyland, J., L. Balthis, I. Karakassis, P. Magni, A. Petrov, J. Shine, O. Vestergaard, and R. Warwick. 2005. Organic carbon content of sediments as an indicator of stress in the marine benthos. *Marine Ecology Progress Series* 295: 91–103.

Jones, M., and E. Pinn. 2006. The impact of a macroalgal mat on benthic biodiversity in Poole Harbour. *Marine Pollution Bulletin* 53: 63–71.

Kamer, K., P. Fong, R.L. Kennison, and K. Schiff. 2004. The relative importance of sediment and water column supplies of nutrients to the growth and tissue nutrient content of the green macroalga *Enteromorpha intestinalis* along an estuarine resource gradient. *Aquatic Ecology* 38: 45–56.

Kristiansen, K., E. Kristensen, and M. Jensen. 2002. The influence of water column hypoxia on the behaviour of manganese and iron in sandy coastal marine sediment. *Estuarine, Coastal and Shelf Science* 55: 645–654.

Largier, J.L., and S. Taljaard. 1991. The dynamics of tidal intrusion, retention and removal of seawater in a bar-built estuary. *Estuarine, Coastal and Shelf Science* 33: 325–338.

Lauringson, V., and J. Kotta. 2006. Influence of the thin drift algal mats on the distribution of macrozoobenthos in Koiguste Bay, NE Baltic Sea. *Hydrobiologia* 554: 97–105.

Lavery, P.S., and A.J. McComb. 1991. Macroalgal–sediment nutrient interactions and their importance to macroalgal nutrition in a eutrophic estuary. *Estuarine, Coastal and Shelf Science* 32: 281–296.

Magni, P. 2003. Biological benthic tools as indicators of coastal marine ecosystems health. *Chemistry and Ecology* 19: 363–372.

Magni, P., D. Tagliapietra, C. Lardicci, L. Balthis, A. Castelli, S. Como, G. Frangipane, G. Giordani, J. Hyland, F. Maltagliati, G. Pessa, A. Rismondo, M. Tataranni, P. Tomassetti, and P. Viaroli. 2009. Animal–sediment relationships: Evaluating the "Pearson–Rosenberg paradigm" in Mediterranean coastal lagoons. *Marine Pollution Bulletin* 58: 478–486.

McLaughlin, K., M. Sutula, L. Busse, S. Anderson, J. Crooks, R. Dagit, D. Gibson, K. Johnston, and L. Stratton. 2013. A regional survey of the extent and magnitude of eutrophication in Mediterranean estuaries of Southern California, USA. *Estuaries and Coasts*. doi:10.1007/s12237-013-9670-8.

Nilsson, H.C., and R. Rosenberg. 1997. Benthic habitat quality assessment of an oxygen stressed fjord by surface and sediment profile images. *Journal of Marine Systems* 11: 249–264.

Norkko, A., and E. Bonsdorff. 1996. Rapid zoobenthic community responses to accumulations of drifting algae. *Marine Ecology Progress Series* 131: 143–157.

Pearson, T.H., and R. Rosenberg. 1978. Macrobenthic succession in relation to organic enrichment and pollution of the marine environment. *Oceanography and Marine Biology. Annual Review* 16: 229–311.

Pelletier, M.C., D.E. Campbell, K.T. Ho, R.M. Burgess, C.T. Audette, and N.E. Detenbeck. 2010. Can sediment total organic carbon and grain size be used to diagnose organic enrichment in estuaries? *Environmental Toxicology and Chemistry* 30: 538–547.

Pihl, L., I. Isaksson, H. Wennhage, and P.O. Moksnes. 1995. Recent increase of filamentous algae in shallow Swedish bays: Effects on the community structure of epibenthic fauna and fish. *Netherlands Journal of Aquatic Ecology* 29: 349–358.

Posey, M.H., T.D. Alphin, L. Cahoon, D.G. Lindquist, M.A. Mallin, et al. 2002. Top–down versus bottom–up limitation in benthic infaunal communities: direct and indirect effects. *Estuaries* 25: 999–1014.

Pusceddu, A., A. Dell'Anno, M. Fabiano, and R. Danovaro. 2009. Quantity and bioavailability of sediment organic matter as signatures of benthic trophic status. *Marine Ecology Progress Series* 375: 41–52.

Qian, S.S., R.S. King, and C.J. Richardson. 2003. Two statistical methods for the detection of environmental thresholds. *Ecological Modelling* 166: 87–97.

Raffaelli, D., S. Hull, and H. Milne. 1989. Long-term changes in nutrients, weed mats and shorebirds in an estuarine system. *Cahiers de Biologie Marine* 30: 259–270.

Raffaelli, D., J. Limia, S. Hull, and S. Pont. 1991. Interactions between the amphipod *Corophium volutator* and macroalgal mats on estuarine mudflats. *Journal of the Marine Biological Association of the United Kingdom* 71: 899–908.

Resilience Alliance and Santa Fe Institute. 2004. Thresholds and alternate states in ecological and social–ecological systems. Resilience Alliance. (Online.) URL: http://www.resalliance.org/index.php?id=183.

Rhoads, D.C., and S. Cande. 1971. Sediment profile camera for *in situ* study of organism–sediment relations. *Limnology and Oceanography* 16: 110–114.

Rhoads, D.C., and J.D. Germano. 1982. Characterization of organism–sediment relationships using sediment profile imaging: An efficient method of Remote Ecological Monitoring of the Seafloor (REMOTS® System). *Marine Ecology Progress Series* 8: 115–128.

Rhoads, D.C., and J.D. Germano. 1986. Interpreting long-term changes in benthic community structure; a new protocol. *Hydrobiologia* 142: 291–308.

Rosenberg, R., A. Gremare, J.-M. Amouroux, and H.C. Nilsson. 2003. Benthic habitats in the northwest Mediterranean characterized by sedimentary organics, benthic macrofauna, and sediment profile images. *Estuarine, Coastal and Shelf Science* 57: 297–311.

Scanlan, C.M., J. Foden, E. Wells, and M.A. Best. 2007. The monitoring of opportunistic macroalgal blooms for the Water Framework Directive. *Marine Pollution Bulletin* 55: 162–171.

Sfriso, A., A. Marcomini, and B. Pavoni. 1987. Relationships between macroalgal biomass and nutrient concentrations in a hypertrophic area of the Venice Lagoon Italy. *Marine Environmental Research* 22: 297–312.

Stoddard, J., D.P. Larsen, C.P. Hawkins, R.K. Johnson, and R.H. Norris. 2006. Setting expectations for the ecological condition of streams: The concept of reference condition. *Ecological Applications* 16: 1267–1276.

Sutula M. 2011. Review of Indicators for Development of Nutrient Numeric Endpoints in California Estuaries. 2011. M Sutula. Technical Report 646. Southern California Coastal Water Research Project. Costa Mesa, CA. www.sccwrp.org/Documents/TechnicalReports.aspx

Teal, L.R., E.R. Parker, G. Fones, and M. Solan. 2009. Simultaneous determination of in situ vertical transitions of color, pore-water metals, and visualization of infaunal activity in marine sediments. *Limnology and Oceanography* 54: 1801–1810.

Teal, L.R., E.R. Parker, and M. Solan. 2010. Sediment mixed layer as a proxy for benthic ecosystem process and function. *Marine Ecology Progress Series* 414: 27–40.

Valiela, I., K. Foreman, M. LaMontagne, D. Hersh, J. Costa, P. Peckol, B. DeMeo-Anderson, C. D'Avanzo, M. Babione, C.-H. Sham, J. Brawley, and K. Lajtha. 1992. Couplings of watersheds and coastal waters: Sources and consequences of nutrient enrichment in Waquoit Bay, Massechusetts. *Estuaries* 15: 443–457.

Valiela, I., J. McClelland, J. Hauxwell, P.J. Behr, D. Hirsch, and K. Foreman. 1997. Macroalgal blooms in shallow estuaries: Controls and ecophysiological and ecosystem consequences. *Limnology and Oceanography* 42: 1105–1118.

Viaroli, P., R. Azzoni, M. Bartoli, G. Giordani, M. Naldi, and D. Nizzoli. 2010. Primary productivity, biogeochemical buffers and factors controlling trophic status and ecosystem processes in Mediterranean coastal lagoons: A synthesis. *Advances in Oceanography and Limnology* 1: 271–293.

Zaldivar, J.-M., A.C. Cardoso, P. Viaroli, A. Newton, R. deWit, C. Ibanez, S. Reizopoulou, F. Somma, A. Razinkovas, A. Basset, M. Jolmer, and N. Murray. 2008. Eutrophication in transitional waters: An overview. *Transitional Waters Monographs* 1: 1–78.